Climate Dynamics manuscript No.
(will be inserted by the editor)

Seven–eight year oscillatory mode of climate variability and its coherence with geomagnetic activity from stratosphere to troposphere

Milan Paluš · Dagmar Novotná

Received: date / Accepted: date

Abstract Phase coherence between geomagnetic activity and temperature variability from stratosphere to troposphere is quantified and statistically tested in the oscillatory mode with the period 7–8 years using the ERA-40/ERA-Interim and NCEP/NCAR reanalysis monthly air temperature data. Conditional phase coherence is used to identify the North Atlantic Oscillation (NAO) as a mediator transferring the geomagnetic influence from the stratosphere to the troposphere and near-surface air temperature. Cross-frequency phase–amplitude causal coupling is evaluated in daily surface air temperature using the conditional mutual information in order to understand the role of the 7–8 year cycle in the climate variability. Statistically significant causal influence of the phase of the 7–8 year cycle on temperature variability with temporal scales shorter than 12 months is observed. Within a large area of Europe, yearly conditional means of surface air temperature change within the 7–8 year cycle in the range 1.2–1.6 K.

Keywords Climate variability · Geomagnetic activity · Phase synchronization · Conditional dependence · North Atlantic Oscillation · Cross-scale causality

1 Introduction

In order to understand complex processes in atmospheric dynamics and climate evolution, a number of methods for identification of dynamical mechanisms underlying experimental data have recently been developed. In successful attempts to identify trends, oscillatory processes or other deterministic signals in a noisy environment, singular system analysis (SSA) has been applied in analysis of noisy time series such as long-term records of meteorological variables (Ghil et al., 2002).

M. Paluš
Institute of Computer Science, Academy of Sciences of the Czech Republic, Pod vodárenskou věží 2, 182 07 Prague 8 Czech Republic
E-mail: mp@cs.cas.cz

D. Novotná
Institute of Atmospheric Physics, Academy of Sciences of the Czech Republic, Boční II/1401, 141 31 Prague 4, Czech Republic

Allen and Smith (1996) introduced the Monte Carlo SSA (MCSSA), a statistical method in which eigenvalues (variance) of the SSA modes are tested using a numerical model reflecting a null hypothesis describing background noise in the analyzed data. Paluš and Novotná (2004) proposed enhanced MCSSA (EMCSSA) as a method for discerning weak dynamical modes with higher regularity or dynamical memory from false oscillatory modes obtained from band-pass SSA-filtered noise. Using the EMCSSA for analysis of solar, geomagnetic and climate-related data, Paluš and Novotná (2007) detected and statistically confirmed existence of several oscillatory modes with different periods. In particular, the oscillatory modes with the period 7–8 years have been found in climate (NAO index, near-surface air temperature from mid-latitude European stations), as well as in solar and geomagnetic data.

Statistical evidence for the presence of oscillatory modes with close periods in solar/geomagnetic and climate data opens a possibility to apply methods of phase synchronization analysis (Pikovsky et al., 2001; Paluš and Novotná, 2006) as a novel tool for inferring interactions from noisy and nonstationary data and to contribute to the renewed interest in the field of Sun–climate relations (Haigh, 2003; De Jager, 2005; Lu et al., 2007; Rind et al., 2008; Lockwood, 2009; Gray et al., 2010; Lockwood et al., 2010; Lockwood, 2012). In order to detect and understand responses to solar forcing, many authors search for relationships between temperature data and solar activity, or quantities closely related to the solar activity. Besides the well-known sunspot numbers, the aa index characterizing the geomagnetic activity provides the longest data set of solar proxies which goes back to 1868 (Mayaud, 1972). Relevance of geomagnetic activity in investigation of climate response to solar activity is noticed by several authors, e.g. Usoskin et al. (2005); De Jager and Usoskin (2006).

Indeed, Paluš and Novotná (2009) observed statistically significant phase coherence, beginning from the 1950's, among oscillatory modes with the period of approximately 7–8 years extracted from the monthly time series of sunspot numbers, geomagnetic activity aa index, North Atlantic Oscillation (NAO) index and near-surface air temperature from several mid-latitude European stations.

Empirical evidence suggests that the response to solar signal is not homogenously distributed over the atmosphere, but it shows latitudinal, longitudinal and altitudinal dependence. While the influence of the solar signal in the stratosphere is documented (Labitzke, 2003; Gray et al., 2010), observations of the tropospheric responses to the solar variability are more ambiguous. Besides the geographical complexity, the dynamical coupling between the stratosphere and troposphere remains poorly understood (Rind et al., 2008; Simpson et al., 2009).

Using the ERA-40/ERA-Interim and NCEP/NCAR reanalysis monthly temperature data, in this study we evaluate phase coherence in the oscillatory mode with the period 7–8 years between geomagnetic activity and temperature variability from the stratosphere to the troposphere. Conditional phase coherence is used to identify the NAO as a mediator transferring the geomagnetic influence from the stratosphere to the troposphere and near-surface air temperature. In order to understand the role of the 7–8 year cycle in the climate variability, cross-frequency phase–amplitude causal coupling is evaluated using the conditional mutual information and a statistically significant influence of the phase of the 7–8 year cycle on variability with temporal scales shorter than 12 months is observed in daily surface air temperature data. Within a large area of Europe, yearly conditional means of surface air temperature change within the 7–8 year cycle in the range 1.2–1.6 K.

2 Methods

2.1 Phase dynamics and phase synchronization

Oscillatory modes extracted from climate variability and geomagnetic activity can be considered as recordings of evolution of dynamical systems. Suppose that evolution of a system is dominated by (quasi-)oscillatory dynamics, then its state can be described by its instantaneous phase ϕ (Pikovsky et al., 2001). For an experimental time series such as long-term recording of air temperature, NAO index or aa index, the phase ϕ can be obtained using the analytic signal concept of Gabor (1946). For an arbitrary time series $s(t)$ the analytic signal $\psi(t)$ is a complex function of time defined as

$$\psi(t) = s(t) + i\hat{s}(t) = A(t)e^{i\phi(t)}. \tag{1}$$

The instantaneous phase $\phi(t)$ of the signal $s(t)$ is then

$$\phi(t) = \arctan\frac{\hat{s}(t)}{s(t)}, \tag{2}$$

and its analytic amplitude is

$$A(t) = \sqrt{s(t)^2 + \hat{s}(t)^2}. \tag{3}$$

There are several ways how to determine the imaginary part $\hat{s}(t)$ of the analytic signal $\psi(t)$. In the standard approach of Gabor (1946), $\hat{s}(t)$ is given by (discrete) Hilbert transform of $s(t)$ (Rosenblum et al., 1996; Paluš, 1997; Pikovsky et al., 2001). Since the Hilbert transform is a unit gain filter at each frequency, broadband signals should be pre-filtered to the frequency band of interest. The approach used in this study is based on wavelet transform (Torrence and Compo, 1998). Applying a continuous complex wavelet transform (CCWT thereafter) directly to time series $s(t)$, the complex coefficients related to the scale (frequency) of the studied oscillatory process can directly be used in Eq. (2) and (3) for the estimation of the phase $\phi(t)$ and the amplitude $A(t)$, respectively. The CCWT provides both the band-pass filtering of the signal and the estimation of the instantaneous phase and amplitude.

Since the instantaneous phase ϕ of an oscillatory system describes its states, phases ϕ_1 and ϕ_2 of two systems can be used to infer their interactions. The form of interaction of two systems depends on the strength of coupling between the two systems. From some coupling strength two dynamical systems become synchronized, i.e., their states are equivalent (Pikovsky et al., 2001).

The simplest case of oscillatory processes are periodic self-sustained oscillators. In such a case synchronization appears as phase locking, i.e., the phase difference $\Delta\phi(t) = \phi_1(t) - \phi_2(t)$ is constant. Real-world phenomena are more complex and their observation is corrupted by noise. In the case of complex and noisy oscillatory processes fluctuations of the phase difference typically occur even in their synchronized state. Therefore, the phenomenon of phase synchronization is defined by the criterion that the absolute values of $\Delta\phi$ are bounded (Rosenblum et al., 1996). If the instantaneous phases are not represented as cyclic functions in the interval $[0, 2\pi)$ or $[-\pi, \pi)$, but as monotonously increasing functions on the whole real line, then also the instantaneous phase difference $\Delta\phi(t)$ is defined on the real line and is an unbounded (increasing or decreasing) function of time for asynchronous (independent) systems. In this representation epochs of phase synchronization (or coherence) appear as plateaus in $\Delta\phi(t)$ vs. time plots. In order to obtain statistical evidence that such a plateau did not occur by chance, but due to phase synchronized dynamics of the observed systems, we need a quantitative characterization of dependence of the phases. In this study we follow Paluš (1997) and use a dependence measure defined in information theory: The mutual information $I(X;Y)$ of two random variables X and Y is given by

$$I(X;Y) = H(X) + H(Y) - H(X,Y), \tag{4}$$

where the entropies $H(X)$, $H(Y)$, $H(X,Y)$ are defined in the standard way according to Shannon (Cover and Thomas, 1991). The involved variables are the instantaneous phases ϕ_1 and ϕ_2, now considered as the cyclic functions on the interval $[0, 2\pi)$. Their mutual information is defined as

$$I(\phi_1, \phi_2) = \int_0^{2\pi}\int_0^{2\pi} p_{1,2}(\phi_1, \phi_2) \log \frac{p_{1,2}(\phi_1, \phi_2)}{p_1(\phi_1)p_2(\phi_2)} d\phi_1 d\phi_2, \tag{5}$$

where $p_1(\phi_1)$ and $p_2(\phi_2)$ are probability distributions of the phases ϕ_1 and ϕ_2, respectively, and $p_{1,2}(\phi_1, \phi_2)$ is their joint distribution.

Mutual information $I(\phi_1, \phi_2)$ is equal to zero if and only if the variables ϕ_1 and ϕ_2 are statistically independent, i.e., $p_{1,2}(\phi_1, \phi_2) = p_1(\phi_1)p_2(\phi_2)$. If there is no interaction between the two oscillatory systems, the independent phases generate a homogeneous distribution of the points (ϕ_1, ϕ_2) in the phase plane $(0, 2\pi) \times (0, 2\pi)$ and $I(\phi_1, \phi_2) = 0$; while for the phase synchronization, i.e., a mutual dependence of the phases, $I(\phi_1, \phi_2) > 0$ holds. Estimates of information-theoretic functionals from empirical distributions always give non-zero values. Therefore for reliable detection of phase synchronization in experimental data it is necessary to establish that $I(\phi_1, \phi_2) > 0$ with a statistical significance.

2.2 Statistical testing

We follow Paluš and Novotná (2006) and apply a statistical testing approach using numerically generated surrogate data that have the same frequency spectra (amplitudes of Fourier coefficients) as the original data, but their Fourier phases are randomized independently for each time series. Thus any dependence between the series, present in the original tested data, is removed in the surrogate data. However, the autocorrelations (serial correlations) of individual series are preserved. Ebisuzaki (1997) advocates an equivalent approach to test crosscorrelations in serially correlated data. Paluš (2007) presents a more general discussion regarding the hypothesis testing procedures using the surrogate data techniques and demonstrates that the famous correlation between the sunspot numbers and the number of the Republican members of the US senate is not statistically significant, just a correct testing approach should be applied.

In this testing approach a pair of time series underwent the CCWT yielding the instantaneous phases ϕ_1 and ϕ_2 and their mutual information $I(\phi_1, \phi_2)$, referred to in the following as I_0, is computed. The original time series are used as the input into the surrogate data randomization procedure and a number of independent realizations of the surrogate time series is produced. Each surrogate pair undergoes the CCWT yielding the instantaneous phases ϕ_1 and ϕ_2 and the mutual information $I(\phi_1, \phi_2)$. The latter are summarized as the mean surrogate mutual information $\bar{I}_s$ and the standard deviation σ_s. The statistical significance of the original value I_0 can be inferred using the z-score $z = (I_o - \bar{I}_s)/\sigma_s$. If we are able to generate a large number of surrogate replications (e.g. 1000), we can estimate empirical distribution of the surrogate $I(\phi_1, \phi_2)$ values, compute the cumulative histogram and the distribution percentiles. Then, if we find, e.g., that the I_0 value is greater than the value for the 95th percentile, we directly have the statistical significance $p < 0.05$ for the tested I_0 value.

2.3 Conditional dependence

Considering three random variables X, Y and Z we can extend the definition (4) and define the conditional mutual information

$$I(X;Y|Z) = H(X|Z) + H(Y|Z) - H(X,Y|Z), \tag{6}$$

where $H(X|Z) = H(X,Z) - H(Z)$ is the conditional entropy of X given Z; other two terms are analogously defined. For Z independent of X and Y the equality

$$I(X;Y|Z) = I(X;Y) \tag{7}$$

holds. By a simple manipulation we obtain

$$I(X;Y|Z) = I(X;Y;Z) - I(X;Z) - I(Y;Z). \tag{8}$$

The conditional mutual information $I(X;Y|Z)$ characterizes the "net" dependence between X and Y without a possible influence of another variable, Z. In full analogy we can extend the definition (5) using the phases ϕ_i, $i = 1,2,3$ and use the conditional mutual information in order to discern phase coherence due to a direct interactions of two systems from a phase coherence mediated by another dynamical phenomenon.

2.4 Cross-frequency phase–amplitude causality

Let $\{x(t)\}$ and $\{y(t)\}$ be time series considered as realizations of stationary, ergodic stochastic processes $\{X(t)\}$ and $\{Y(t)\}$, respectively, $t = 1,2,3,\ldots$. The mutual information $I(y(t);x(t+\tau))$ measures the average amount of information contained in the process $\{Y\}$ about the process $\{X\}$ in its future τ time units ahead (τ-future thereafter). It is possible, however, that this measure also contains information about the τ-future of the process $\{X\}$ contained in this process itself. This is the case if the processes $\{X\}$ and $\{Y\}$ are not independent, i.e., if $I(X;Y) > 0$.

The conditional mutual information $I(Y;X_\tau|X)$, where X_τ refers to process $\{X\}$ shifted τ time units ahead, estimates the "net" information about the τ-future of the process $\{X\}$ contained in the process $\{Y\}$. Paluš (2007) discusses the problem of causality detection in detail, and show that in time series representation the functional $I(y(t);x(t+\tau)|x(t),x(t-\eta),\ldots x(t-m\eta))$ can be used for inference of causal influence of $\{Y\}$ on $\{X\}$. The conditioning variables depend on memory/dimensionality of the process $\{X\}$. Hlaváčková-Schindler et al. (2007) discuss the causality detection problem in detail, and describe a number of methods for estimation of related information-theoretic functionals. Molini et al. (2010) use the equivalent information-theoretic approach in order to infer causality across rainfall time scales.

Here we study possible influence of the phase ϕ_1 of slow oscillations on amplitude A_2 of higher-frequency variability of the same process/time series, using the functional $I(\phi_1(t);A_2(t+\tau)|A_2(t),A_2(t-\eta),\ldots,A_2(t-m\eta))$. For statistical evaluation the surrogate data strategy (Sec. 2.2) is used.

3 Data

As an example of station data we use daily and monthly mean values of surface air temperature (SAT) from Prague–Klementinum (longitude 14° 25'E, latitude 50° 05'N), from the period 1900–2007. The main focus of the analyses is on the gridded monthly air temperature from the reanalysis sets; we use the term "ERA" for the concatenation of the period 1958–1988 from the ERA-40 data (Uppala et al., 2005), and the period 1989–2008 from the ERA-Interim set (Dee et al., 2011). The monthly air temperature data from the NCEP/NCAR (Kalnay et al., 1996) reanalysis are also used from the period 1958–2008, for comparability of the two data sets. For both the sets the grid of 2.5° x 2.5° is used.

The monthly NAO index was obtained from http://www.cru.uea.ac.uk/cru/data/. The geomagnetic aa-index was obtained from World Data Centre for Solar-Terrestrial Physics, Chilton, http://www.ukssdc.ac.uk/data/wdcc1/wdc_menu.html.

4 Results

4.1 Phase difference plateaus from 1950's to 1990's

Exploring the instantaneous phases of the oscillatory mode obtained using the CCWT with the central wavelet frequency, related to the period of 96 months, Paluš and Novotná (2009) demonstrated that the instantaneous phase difference $\Delta\phi(t)$ between the geomagnetic aa index and SAT from several European stations forms a plateau starting in the 1950's. The filtered sunspot numbers brought the same result. Here we focus on the aa index and present $\Delta\phi(t)$ between the aa index and the SAT from the Prague-Klementinum station (Fig. 1, the longest, black curve) together with the SAT from the closest reanalysis grid point (15° 00'E, 50° 00'N) from the NCEP/NCAR (Fig. 1, the red curve) and ERA (Fig. 1, the shortest, blue curve) data. The presentation of Fig. 1 is not only a remainder of the previous results, but, with the help of the recent data extension, it gives us the possibility to discern the end of the phase-coherence epoch from possible

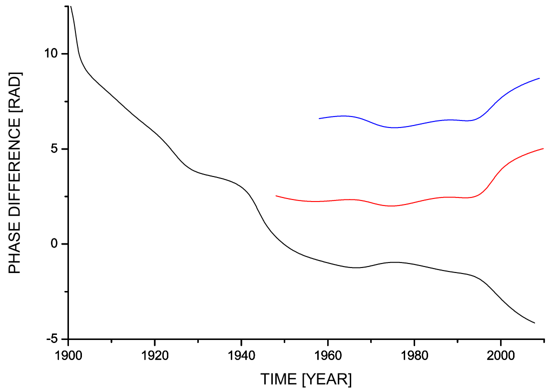

Fig. 1 The instantaneous phase differences between the aa index and SAT from the Prague-Klementinum station (14° 25'E, 50° 05'N) (the longest, black curve), NCEP/NCAR (the red curve) and ERA (the shortest, blue curve) grid point (15° 00'E, 50° 00'N). The oscillatory modes and their phases were obtained using CCWT with the central wavelet period 96 months.

edge effect of the CCWT. Unlike Paluš and Novotná (2009), due to the extended data, we can clearly see that the phase coherence between the climate variability and the geomagnetic activity ends around 1995. Therefore, in all the subsequent analyses, the phase coherence is evaluated in the period 1958–1994.

4.2 Northern Hemisphere SAT phase coherence patterns

Using the Northern Hemisphere near-surface air temperature data from NCEP/NCAR and ERA reanalyses, Paluš and Novotná (2011) observed consistent patterns of areas with marked phase coupling between solar/geomagnetic activity and climate variability in continuous monthly data, independent of the season, however, confined to the temporal scale related to the oscillatory periods about 7–8 years.

In this study we quantify the phase coherence using the mutual information (5) in the period 1958–1994, while Paluš and Novotná (2011) used a different measure and a slightly longer period. Comparable examples of the phase coherence patterns are presented in Fig. 2. Significance levels, based on 1000 realizations of surrogate data, for $I(\phi_1, \phi_2)$ reflecting the phase coherence of the geomagnetic aa index and NCEP/NCAR SAT are illustrated in Fig. 2a. The corresponding significance levels for phase coherence between the NAO index and NCEP/NCAR SAT are mapped in Fig. 2b, for the NAO index and ERA SAT in Fig. 2c.

The areas with the significant phase coherence between SAT and the aa index, in particular, the European areas north of 44° N (Fig. 2a) are confined within the area of the significant phase coherence between SAT and the NAO index (see Fig. 2b for NCEP/NCAR SAT; and Fig. 2c for ERA SAT). This coincidence opens a question about a possible role of the NAO phenomenon in transferring the geomagnetic (and possibly solar) influence to the troposphere close to the Earth surface. We can test such a hypothesis by evaluating the conditional mutual information (8). Note that we always consider the part of climate/geomagnetic

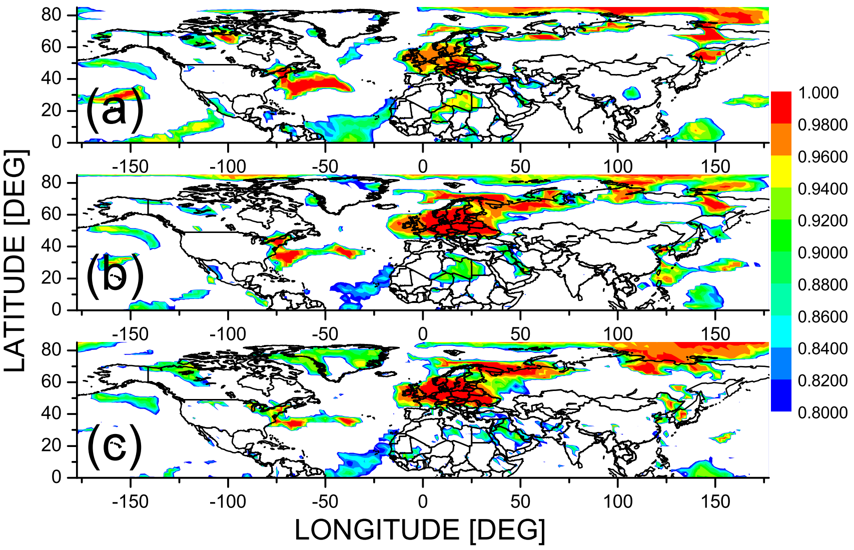

Fig. 2 The significance levels for phase coherence between (a) the geomagnetic aa index and NCEP/NCAR SAT; (b) the NAO index and NCEP/NCAR SAT; and (c) the NAO index and ERA SAT, for the oscillatory modes obtained using CCWT with the central wavelet period 96 months. The color code illustrates the surrogate distribution percentile crossed by the I_0 values, e.g. for 0.96–0.98 (orange) the phase coherence is significant with $p < 0.04$; for 0.98–1.00 (red) with $p < 0.02$.

variability related to the oscillatory modes with the period about 7–8 years, therefore we compute the conditional mutual information $I(\phi_1, \phi_2|\phi_3)$ using the phases of the three variables: the aa index, the NAO index and SAT in each reanalysis gridpoint.

The significance levels for the conditional phase coherence between the geomagnetic aa index and ERA SAT, conditioned on the NAO index are illustrated in Fig. 3a. The phase coherence in the formerly significant European areas almost disappeared due to conditioning on the NAO index. This is a quantitative evidence that the interactions between (a part of) the SAT variability and the geomagnetic activity, extended over Europe, is mediated by the NAO variability. The SAT variability in an area in the Atlantic Ocean and in Northern Asia and Arctic areas either directly interacts with the geomagnetic activity, or a different mediator exists.

In order to check whether the effect of conditioning is not symmetric, in Fig. 3b the significance levels are plotted for the conditional phase coherence between the NAO index and ERA SAT, conditioned on the geomagnetic aa index. The conditioning on the aa index apparently does not change the SAT–NAO coherence, thus the primary character of the interactions between the SAT and NAO variability in the European areas is confirmed.

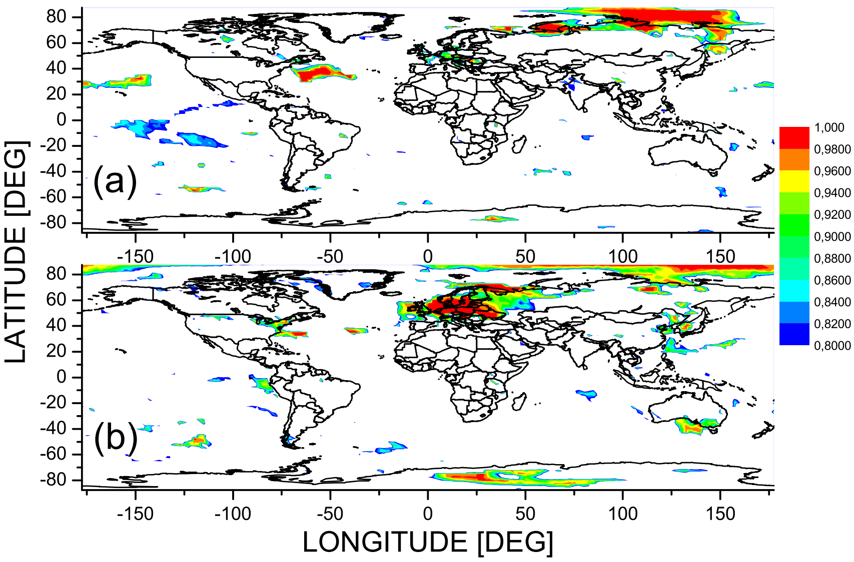

Fig. 3 The significance levels for conditional phase coherence (a) between the geomagnetic aa index and ERA SAT, conditioned on the NAO index; and (b) between the NAO index and ERA SAT, conditioned on the aa index, for the oscillatory modes obtained using CCWT with the central wavelet period 96 months.

4.3 Phase coherence between climate variability and geomagnetic activity from stratosphere to troposphere

In the following we study altitudinal dependence of the patterns of the phase coherence between the air temperature and the geomagnetic activity. Figure 4a presents the significance levels for the phase coherence between the geomagnetic aa index and the air temperature T30 on the isobaric level 30 hPa. In the stratosphere the areas of interactions of the temperature variability and the geomagnetic activity are quite more extended then near the Earth surface.

The significance levels for conditional phase coherence between the geomagnetic aa index and temperature T30, conditioned on the NAO index, are mapped in Fig. 4b. The decrease, comparing to Fig. 4a, is practically negligible. These results support the possibility of direct interactions between temperature/climate variability and the geomagnetic activity in the stratosphere.

The same experiment as in Fig. 4, but for interactions between the stratospheric temperature T30 and the NAO index, with the aa index as the conditioning variable, is presented in Fig. 5. Unlike in the near-surface air temperature, the areas of the significant coherence between the stratospheric air temperature T30 and the NAO index are less extended than the areas of the significant coherence between the aa index and T30. Conditioning on the aa index decreases the NAO–T30 coherence only in some areas. Considering these results we can conclude that in the

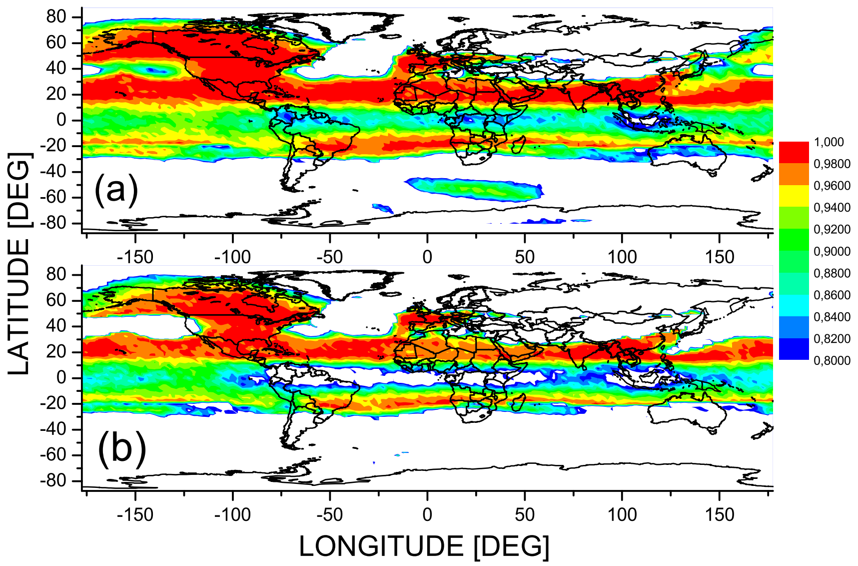

Fig. 4 The significance levels for (a) phase coherence between the geomagnetic aa index and ERA temperature T30 on the isobaric level 30 hPa; (b) conditional phase coherence between the geomagnetic aa index and ERA temperature T30 on the isobaric level 30 hPa, conditioned on the NAO index, for the oscillatory modes obtained using CCWT with the central wavelet period 96 months.

stratosphere there are globally extended areas where the geomagnetic activity and NAO interact with the air temperature independently of each other.

Examples of the patterns of altitudinal dependence of the phase coherence and the conditional phase coherence are illustrated in Figs. 6 and 7 where the slices for the latitude 52.5°N and the longitude 75°E, respectively, are presented. While the most significant areas of the temperature–NAO coherence are almost unaffected by the conditioning on the aa index, the areas of the significant coherence between temperature and the aa index are considerably reduced by conditioning on the NAO index in the tropospheric and near-surface areas. Thus the NAO variability is probably not the sole, but the most important mediator of the geomagnetic and possibly solar influence on the tropospheric and near-surface air temperature variability in the areas under the NAO influence.

4.4 Cross-frequency phase–amplitude coupling in air temperature

All the results presented in the previous sections were obtained for the part of the geomagnetic activity, NAO and air temperature variability related to the oscillatory mode with the period about 7–8 years. This oscillatory phenomenon has been detected by many authors in various climate-related records (see the references in Sec. 5), yet its importance in climate variability is not understood. The simplest, “linear” approach would be to estimate amplitude of this cycle, say, in

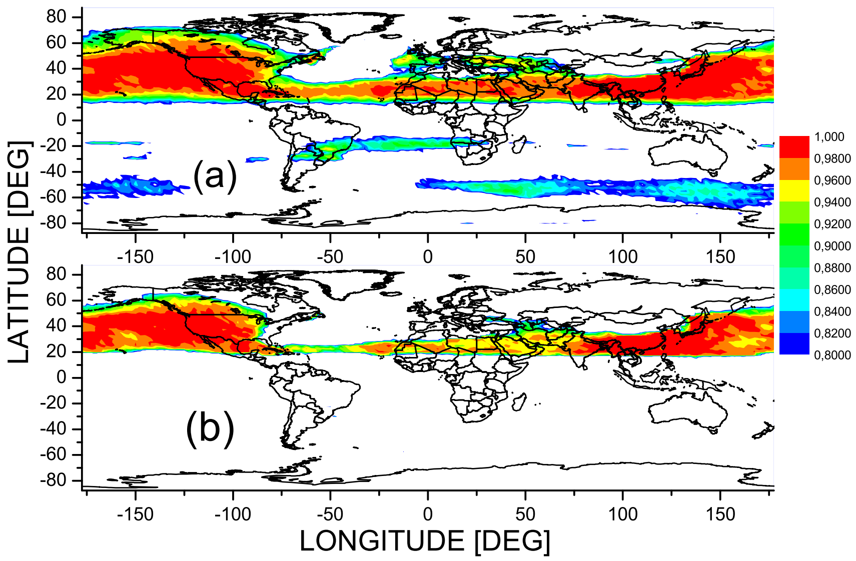

Fig. 5 The significance levels for (a) phase coherence between the NAO index and ERA temperature T30 on the isobaric level 30 hPa; (b) conditional phase coherence between the NAO index and ERA temperature T30 on the isobaric level 30 hPa, conditioned on geomagnetic aa index, for the oscillatory modes obtained using CCWT with the central wavelet period 96 months.

air temperature variability. Technically, however, this is a complicated problem, since the amplitude of cycles extracted by methods such as SSA or wavelet transform depends on particular parameters of the used extraction method. Moreover, Paluš and Novotná (2004) stress that the enhanced MCSSA, used to detect this oscillatory mode, is able to discern from a colored noise background an oscillatory mode which is weak in its variance, but its dynamical regularity and predictability is significantly greater than these properties obtained from band-pass filtered colored noise. Although the broad-band dependence structures in temporal evolution of long-term near-surface air temperature records are well-explained by a linear stochastic model (Paluš and Novotná, 1994), the increased regularity of the dynamics of the 7–8 year mode suggests its nonlinear deterministic origin, stemming probably from nonlinear ocean-atmosphere interactions. These considerations, however, are beyond the scope of this article. For better understanding of the role that the 7–8 year mode may play in the climate variability, we will study possible cross-frequency interactions in the daily near-surface air temperature record from the Prague-Klementinum station.

The cross-frequency coupling, in particular, the cross-frequency phase–amplitude interaction is a phenomenon occurring in complex, multiscale oscillatory processes such as the brain electrical activity (Canolty and Knight, 2010). Typically, the phase of slower oscillations can influence the amplitude and variance of faster oscillations. In order to infer possible causal cross-frequency phase–amplitude influ-

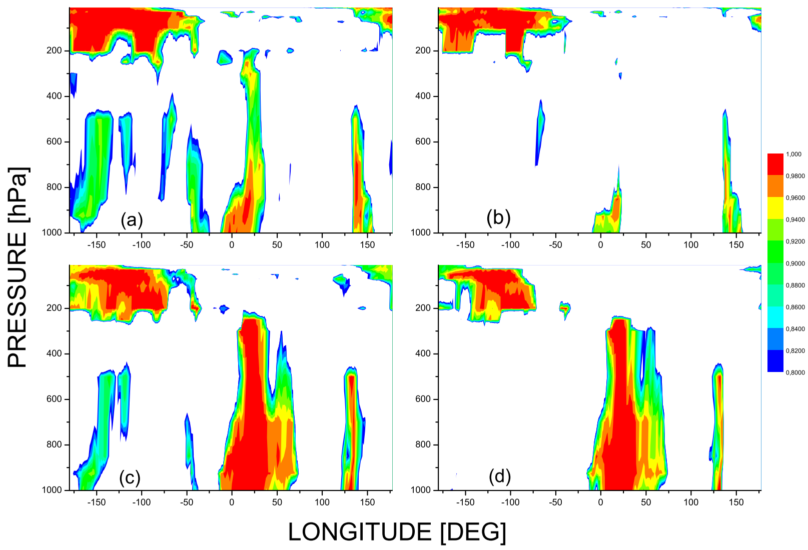

Fig. 6 The significance levels for (a, c) phase coherence and (b,d) for conditional phase coherence between (a) the geomagnetic aa index and temperature; (b) the geomagnetic aa index and temperature conditioned on the aa index; (c) the NAO index and temperature; and (d) the NAO index and temperature conditioned on the aa index, for the oscillatory modes obtained using CCWT with the central wavelet period 96 months, for the latitude 52.5°N, ERA temperature data.

ence, we apply the conditional mutual information $I(\phi_1(t); A_2(t+\tau)|A_2(t), A_2(t-\eta), \ldots, A_2(t-m\eta))$, introduced in Sec. 2.4. This functional is averaged for forward lags τ from 1 to 750 days, while the three-dimensional conditioning variable $A_2(t), A_2(t-\eta), A_2(t-2\eta))$ is used, where the backward lag η is always equal to 1/4 of the period of the slower oscillations characterized by the phase ϕ_1. The results, in the form of z-scores (Sec. 2.2) obtained using 100 surrogate data realizations, are presented in Fig. 8. Considering a normal distribution for conditional mutual information of the surrogate data, we color-code the z-scores for the values greater than two standard deviations (SD) of the surrogate distribution. We can see that phases of oscillatory modes with periods from 6 to 11 years influence variability characterized by the periods around 1 year. There is also some influence of the periods 6–7 years on variability with the periods under 6 months, and of the periods 8–10 years on variability with the periods slightly under 2.5 years. However, the most significant influence (z-scores over 7–9 SD's, colored in orange and red in Fig. 8) is exerted by the cycles with the periods about 7–8 years on the variability characterized by the oscillatory periods under one year (about 0.8 − 0.9 year). This result is a strong quantitative evidence for cross-frequency coupling in temperature records from central Europe in which a particular role is played by the cycle with the period about 7–8 years, influencing the variability on the temporal scales under 12 months. Yet this result does not give us the size of

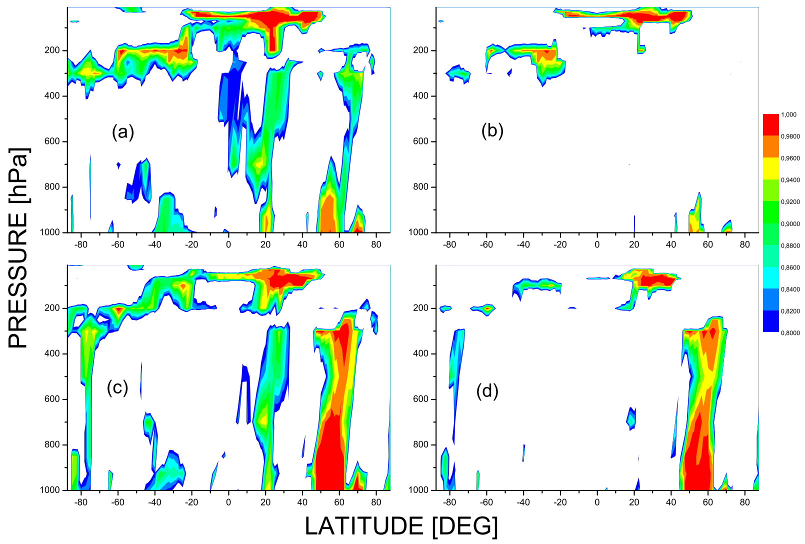

Fig. 7 The significance levels for (a, c) phase coherence and (b,d) for conditional phase coherence between (a) the geomagnetic aa index and temperature; (b) the geomagnetic aa index and temperature conditioned on the aa index; (c) the NAO index and temperature; and (d) the NAO index and temperature conditioned on the aa index, for the oscillatory modes obtained using CCWT with the central wavelet period 96 months, for the longitude 75°E, ERA temperature data.

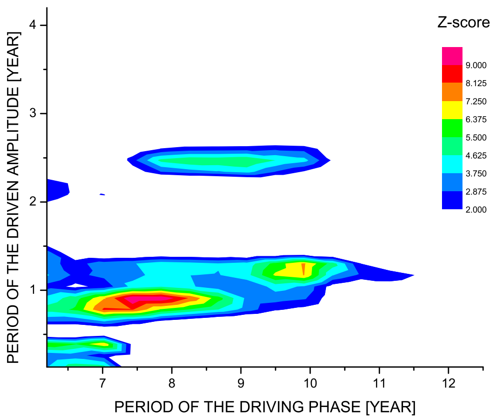

Fig. 8 The z-scores for the conditional mutual information quantifying the causal influence of the phase of slower oscillations (period on abscissa) on the amplitude of the faster variability (oscillatory period on ordinate). Oscillatory phases and amplitudes are extracted using CCWT from the daily surface air temperature (Prague-Klementinum station).

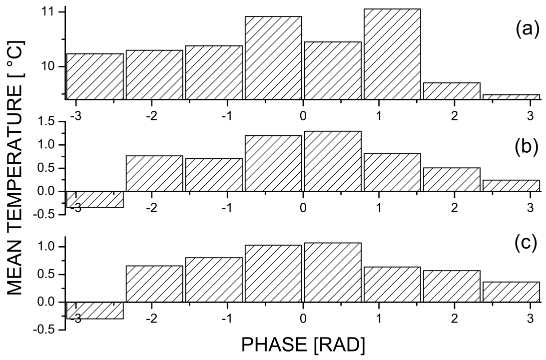

Fig. 9 Conditional means for the Prague-Klementinum (a) daily SAT, (b) daily SAT anomalies, and (c) monthly SAT anomalies, conditioned on the phase of the 7–8 year cycle, obtained for 8 bins equidistantly dividing the interval $[-\pi, \pi)$ of the cyclic phase.

the effect. In order to estimate the latter, we compute conditional means of the daily SAT, conditioned on the phase of the oscillatory mode obtained from the SAT data by using CCWT with the central frequency 8 years. Each SAT sample has assigned a value of the cyclic phase $\phi_1(t) \in [-\pi, \pi)$ of the 7–8 year oscillatory mode. The interval $[-\pi, \pi)$ of the cyclic phase is divided into eight equidistant bins and the conditional SAT means are obtained by averaging the raw SAT values in each of the phase bins. Note that due to the 8 bins for the phase of the 7–8 year cycle, each phase-bin-conditioned mean is also approximately a yearly mean, for each of the 8 different parts of the cycle. In this way we estimate the influence of the 7–8 year cycle on the overall SAT variability. In Fig. 9a we can see that the conditional SAT means range from 9.48 to 11.05°C, i.e. the difference of the conditional SAT means within the 7–8 year cycle is 1.57 K (Prague-Klementinum station). The result in Fig. 9a is obtained from the raw SAT data, including the annual cycle. Since the strongest influence of the 7–8 year cycle is not directly on the annual cycle, but on periods slightly below, let us repeat the computation for the daily SAT anomalies. Now the values in the extremum phase bins are -0.35 and 1.29°C (Fig. 9b). The conditional mean temperature difference within the 7–8 year cycle, without the influence of the annual temperature cycle, is 1.62 K. Using the Prague-Klementinum monthly SAT anomalies (Fig. 9c), the difference is 1.36 K, i.e., the monthly averaging partially attenuates the effect.

Computing in the same way the SAT conditional means and their difference between the bins starting at $-\pi$ and 0 radians (Fig. 9c), now using the monthly reanalysis data we map the SAT conditional mean differences within the 7–8 year cycle for the extratropical Northern Hemisphere (ERA in Fig. 10a, and NCEP/NCAR in Fig. 10b). In agreement with the above station data, these differences are within the 1.2–1.6 K range within a large area of Europe, with a smaller subset with the differences up to 2 K. The effect is apparent also in other areas of the Northern Hemisphere, with a few extrema around 3K.

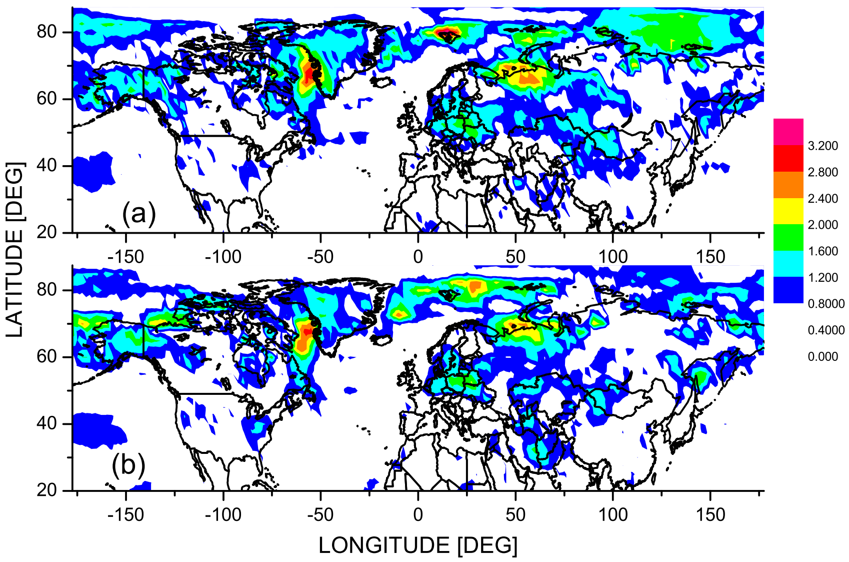

Fig. 10 The maximum conditional mean temperature difference (color-coded in degrees K) within the 7–8 year cycle obtained from monthly (a) ERA, and (b) NCEP/NCAR SAT anomalies in the extratropical Northern Hemisphere.

5 Discussion and conclusion

The pattern of the statistically significant phase coherence between the geomagnetic activity and climate variability in the stratosphere (30 hPa) spans a large area between 30°S and 30°N, in some areas of the Northern Hemisphere expanding over 50°N, or even over 60°N (Fig. 4a). This area is comparable with the pattern of correlation between T30 and the solar activity presented by Gray et al. (2010) and Labitzke (2003). Labitzke (2003) observed a similar extent of areas where the stratospheric temperature and the solar activity interact after restriction to a particular month and a particular phase of the quasibiennial oscillations (QBO), while our results in Fig. 4a have been obtained from continuous monthly data, independently of the season or the QBO phase, however, confined to the temporal scale related to the oscillatory periods about 7–8 years.

In the troposphere and near the surface the geomagnetic influence on the air temperature is apparently weaker. Moreover, the areas with the significant phase coherence between SAT and the aa index, in particular, the European areas north of 44° N (Fig. 2a) are confined within the area of the significant phase coherence between SAT and the NAO index (see Fig. 2b for NCEP/NCAR SAT; and Fig. 2c for ERA SAT). The fact that the response to external (solar, geomagnetic) forcing often has the same spatial structure as, and involves similar eddy mean flow feedbacks to, the dominant pattern of variability, e.g., the annular mode (NAO/AO) signal at middle to high latitudes and the El Niño Southern Oscillation (ENSO) signal at tropical latitudes, is stated by Gray et al. (2010) in their review paper where also references to observations and modeling of the phenomenon are provided. Also, Ruzmaikin and Feynman (2002) suggest that a mechanism of solar influence on climate operates through the excitation of the North Annular Mode. Using the concept of conditional phase coherence, in this study we provide a quantitative evidence that the geomagnetic, and possibly, solar influence on tropospheric and near-surface climate variability is mediated by the dominant pattern of atmospheric variability in the affected areas - the North Atlantic Oscillation. Note that we study the variability in the temporal scales related to the oscillatory periods 7–8 years. According to Feliks et al. (2010) the 7–8 year cycle might be induced by an oscillation of similar period in the position and strength of the Gulf Stream's sea surface temperature front in the North Atlantic. The 7–8 year variability in the Gulf Stream, in turn, has been attributed to an oscillatory gyre mode of the North Atlantics wind-driven circulation. Thus the 7–8 year cycle influences climate variability in areas influenced by, or teleconnected to NAO. In these areas, NAO is also the mediator transferring the solar/geomagnetic influence from the stratosphere to the troposphere and the surface air temperature. It is possible that studying variability in temporal scales typical for a different dominant mode of atmospheric variability, say ENSO (periods 4–6 years), equivalent results for ENSO and the areas affected by ENSO could be found.

The temporal scale related to the oscillatory periods 7–8 years, used in the analyses of this study, was not chosen arbitrarily but resulted from the long-term study of Paluš and Novotná (2004, 2006, 2009, 2011) who detected the 7–8 year oscillatory cycle in solar and geomagnetic activity and climate variability. The observations of Paluš and Novotná (2004, 2006, 2009, 2011) are not isolated in the scientific literature. Gámiz-Fortis and Sutton (2007) obtained a quasi-periodic, similar to 7-year signal in sea surface temperature and sea surface salinity using a control integration of the HadCM3 coupled climate model. Plaut et al. (1995) detected an oscillatory component with the period 7.7 years in 335 years long central England temperature record. Using global sea-surface temperature fields, Moron et al. (1998) observed 7–8 year oscillations involving the entire double-gyre circulation of the North Atlantic. Gámiz-Fortis et al. (2002) detected oscillations with the period 7.7 years in the winter NAO index. Jevrejeva and Moore (2001) report the oscillatory mode with the period of 7.8 years in the NAO, in the Arctic Oscillation, in the Uppsala winter near-surface air temperature, as well as in the Baltic Sea ice annual maximum extent. Unal and Ghil (1995) and Jevrejeva et al. (2006) observed oscillations with periods of 7 – 8.5 years in a number of sea level records. Da Costa and Colin de Verdiere (2002) detected oscillations with the period 7.7 years in interactions of the sea surface temperature and the sea level pressure. Feliks et al. (2010) report the significant oscillatory mode with the 7.8 year period in the Nile River record, the Jerusalem precipitation, tree rings and in the NAO index.

In spite of all these results the actual role of the 7–8 year mode in climate variability was not adequately quantified yet. Using the information-theoretic approach to cross-frequency causality we demonstrated that the phase of the 7–8 year cycle influences variability on temporal scales shorter than 12 months. The influence of the 7–8 year cycle on the overall SAT variability is quantified by changes in the conditional yearly means within the range 1.2–1.6K in large areas of Europe and the Northern Hemisphere. There are also smaller areas where this difference reaches over 3K, however these extremum values should be taken with cautions and a possible influence of data errors and instrumental nonstationarities should be assessed. In any case the oscillatory phenomena with the period 7–8 years represent an important part of climate variability and should be taken into account in understanding and modeling climate change in large areas of the Northern Hemisphere.

Acknowledgements This study was supported by the Czech Science Foundation, Project No. P103/11/J068.

References

Allen MR, Smith LA (1996) Monte Carlo SSA: Detecting irregular oscillation in the presence of colored noise. J Clim 9(12):3373–3404

Canolty RT, Knight RT (2010) The functional role of cross-frequency coupling. Trends in cognitive sciences 14(11):506–515. doi:10.1016/j.tics.2010.09.001.

Cover TM, Thomas JA (1991) Elements of Information Theory. J. Wiley & Sons, New York

Da Costa ED, de Verdiere AC (2002) The 7.7-year North Atlantic Oscillation. Q J R Meteorol Soc 128:797-817. doi:10.1256/0035900021643692.

Dee DP et al. (2011) The ERA-Interim reanalysis: configuration and performance of the data assimilation system. Q J R Meteorol Soc 137:553–597. doi:10.1002/qj.828.

De Jager C (2005) Solar forcing of climate. 1: Solar variability. Space Sci Rev 120:197-241. doi:10.1007/s11214-005-7046-5.

De Jager C, Usoskin IG (2006) On possible drivers of Sun-induced climate changes. J Atmos Sol-Terr Phys 68:2053-2060. doi:10.1016/j.jastp.2006.05.019.

Ebisuzaki W (1997) A method to estimate the statistical significance of a correlation when data are serially correlated. J Clim 10:2147–2153

Feliks Y, Ghil M, Robertson AW 2010 Oscillatory Climate Modes in the Eastern Mediterranean and Their Synchronization with the North Atlantic Oscillation. J Clim 23:4060–4079. doi:10.1175/2010JCLI3181.1.

Gabor D (1946) Theory of Communication. J IEE London 93(3):429–457

Gámiz-Fortis S R, Pozo-Vázques D, Esteban-Parra MJ, Castro-Díez Y (2002) Spectral characteristics and predictability of the NAO assessed through Singular Spectral Analysis. J Geophys Res 107 D23:4685. doi:10.1029/2001JD001436.

Gámiz-Fortis SR, Sutton RT (2007) Quasi-periodic fluctuations in the Greenland-Iceland-Norwegian Seas region in a coupled climate model. Ocean Dyn 57(6):541-557. doi:10.1007/s10236-007-0116-3.

Ghil MR, Allen M, Dettinger MD et al. (2002) Advanced spectral methods for climatic time series. Rev Geophys 40 (1):1003. doi: 10.1029/2000RG000092.

Gray, LJ, Beer J, Geller M et al. (2010) Solar influences on climate. Rev Geophys 48:RG4001. doi:10.1029/2009RG000282.

Haigh JD (2003) The effects of solar variability on the Earth‘s climate. Phil Trans R Soc Lond A 361:95-111. doi:10.1098/rsta.2002.1111.

Hlaváčková-Schindler K, Paluš M, Vejmelka M, Bhattacharya J (2007) Causality detection based on information-theoretic approaches in time series analysis. Phys Rep 441:1–46. doi:10.1016/j.physrep.2006.12.004.

Jevrejeva S, and Moore JC (2001) Singular Spectrum Analysis of Baltic Sea ice conditions and large-scale atmospheric patterns since 1708. Geophys Res Lett 28(23):4503-4506. doi:10.1029/2001GL013573.

Jevrejeva S, Grinsted A, Moore JC, Holgate S (2006) Nonlinear trends and multiyear cycles in sea level records. J Geophys Res 111:C09012. doi:10.1029/2005JC003229.

Kalnay E, Kanamitsu M, Kistler R et al. (1996) The NCEP/ NCAR 40-year re-analysis project. Bull Am Meteorol Soc 77:437–471. doi: 10.1175/1520-0477(1996)077

Labitzke K (2003) The global signal of the 11-year solar cycle in the atmosphere: When do we need the QBO? Meteorol Z 12:209-216. doi:10.1127/0941-2948/2003/0012-0211.

Lockwood M (2009) Recent changes in solar outputs and the global mean surface temperature. III. Analysis of contributions to global mean air surface temperature rise. Proc R Soc A 464:1387-1404. doi:10.1098/rspa.2007.0348.

Lockwood M (2012) Solar Influence on Global and Regional Climates. Surv Geophys doi:10.1007/s10712-012-9181-3.

Lockwood M, Bell C, Woolings T, Harrison RG, Gray LJ, Haigh JD (2010) Top–down solar modulation of climate: evidence for centenial–scale change. Env Res Lett 5:034008, doi:10.1088/1748-936-26/5/3/034008.

Lu H, Jarvis MJ, Graf HF, Young PC, and Horne RB (2007) Atmospheric temperature response to solar irradiance and geomagnetic activity. J Geophys Res 112:D11109. doi:10.1029/2006JD007864.

Mayaud PN (1972) The aa indices: a 100year series characterizing the magnetic activity. J Geophys Res 77(34):6870–6874

Molini A, Katul GG, Porporato A (2010) Causality across rainfall time scales revealed by continuous wavelet transforms. J Geophys Res 115:D14123. doi:10.1029/2009JD013016.

Moron V, Vautard R, Ghil M (1998) Trends, interdecadal and interannual oscillations in global sea-surface temperatures. Clim Dynam 14(7–8):545-569. doi:10.1007/s003820050241.

Paluš M (1997) Detecting phase synchronization in noisy systems. Phys Lett A 235:341-351. doi:10.1016/S0375-9601(97)00635-X.

Paluš M (2007) From nonlinearity to causality: statistical testing and inference of physical mechanisms underlying complex dynamics. Contemp Phys 48(6):307–348. doi10.1080/00107510801959206.

Paluš M, Novotná D (1994) Testing for nonlinearity in weather records. Phys Lett A 193:67-74. doi:10.1016/0375-9601(94)91002-2.

Paluš M, Novotná D (2004) Enhanced Monte Carlo Singular System Analysis and detection of period 7.8 years oscillatory modes in the monthly NAO index and temperature records Nonlin Processes Geophys 11:721–729. doi:10.5194/npg-11-721-2004.

Paluš M, Novotná D (2006) Quasi-biennial oscillations extracted from the monthly NAO index and temperature records are phase-synchronized. Nonlin Processes Geophys 13:287–296. doi:10.5194/npg-13-287-2006.

Paluš M, Novotná D (2007) Common oscillatory modes in geomagnetic activity, NAO index and surface air temperature records. J Atmos Sol-Terr Phys 69:2405-2415. doi:10.1016/j.jastp.2007.05.009.

Paluš M, Novotná D (2009) Phase-coherent oscillatory modes in solar and geomagnetic activity and climate variability. J Atmos Sol-Terr Phys 71:923-930. doi:10.1016/j.jastp.2009.03.012.

Paluš M, Novotná D (2011) Northern Hemisphere patterns of phase coherence between solar/geomagnetic activity and NCEP/NCAR and ERA40 near-surface air temperature in period 7–8 years oscillatory modes. Nonlin Processes Geophys 18:1–10. doi:10.5194/npg-18-1-2011.

Pikovsky A, Rosenblum M, Kurths J (2001) Synchronization. A Universal Concept in Nonlinear Sciences. Cambridge University Press, Cambridge

Plaut, G, Ghil M, Vautard R (1995) Interannual and interdecadal variability in 335 years of central England temperatures. Science 268:710–713

Rind D, Lean J, Lerner J, Lonergan P, Leboissitier A (2008) Exploring the stratospheric/tropospheric response to solar forcing. J Geophys Res A 113:D24103. doi:10.1029/2008JD010114.

Rosenblum MG, Pikovsky AS, and Kurths J (1996) Phase synchronization of chaotic oscillators. Phys Rev Lett 76:1804-1807. doi:10.1103/PhysRevLett.76.1804.

Ruzmaikin A, Feynman J (2002) Solar influence on a major mode of atmospheric variability. J Geophys Res 107:4209. doi:10.1029/2001JD001239.

Simpson IR, Blackburn M, Haigh JD (2009) The role of eddies in driving the tropospheric response to stratospheric heating perturbations. J Atmos Sci 66(5):1347-1365. doi:10.1175/2008JAS2758.1.

Torrence C, Compo GP (1998) A practical guide to wavelet analysis. Bull Am Meteorol Soc 79(1):61-78. doi:10.1175/1520-0477(1998)079<0061:APGTWA>2.0.CO;2.

Unal YS, Ghil M (1995) Interannual and interdecadal oscillation patterns in sea level. Clim Dynam 11:255-278

Uppala SM et al. (2005) The ERA-40 re-analysis. Q J R Meteorol Soc 131:2961–3012. doi: 10.1256/qj.04.176.

Usoskin IG, Schussler M, Solanki SK, Mursula K (2005) Solar activity, cosmic rays, and Earth's temperature. A millenium-scale comparison. J Geophys Res 110:A10102. doi:10.1029/2004JA010946.